archives
of thermodynamics
Vol. **39**(2018), No. 2, 73–95
DOI: 10.1515/aoter-2018-0013

Hybrid cascade refrigeration systems for refrigeration and heating

K. MEGDOULI[1,2*]
Y. EZZAALOUNI[1]
E. NAHDI[1]
A. MHIMID[2]
L. KAIROUANI[1]

[1] Unité de Recherche Energétique et Environnent, Ecole National d'ingénieur de Tunis 37 Le Belvédčre Tunis, Tunisie.

[2] Laboratoire d'Études des Systèmes Thermiques et Énergétiques Ecole National d'ingénieur de Monastir Avenue Ibn El Jazzar, 5019 Monastir, Tunisie

Abstract In this study a cooling ejector cycle coupled to a compression heat pump is analyzed for simultaneous cooling and heating applications. In this work, the influence of the thermodynamic parameters and fluid nature on the performances of the hybrid system is studied. The results obtained show that this system presents interesting performances. The comparison of the system performances with hydrofluorocarbons (HFC) and natural fluids is made. The theoretical results show that the a low temperature refrigerant R32 gives the best performance.

Keywords: Ejector cycle; Heat pump; Comparison; Refrigerant; Coefficient of performance; Irreversibility; Exergy loss; Second law efficiency

Nomenclature

COP	–	coefficient of performance
C_p	–	specific heat of gas at constant pressure, kJ/kgK
c	–	compressor

*Corresponding Author. Email: karima.megdouli@gmail.com

D – diameter of the mixing chamber, m
d – diameter the primary nozzle exit, m
d_D – diameter at the diffuser exit, m
d_* – diameter of the primary nozzle throat, m
F – coefficient of wall friction
f_x – friction force per unit of mass, N/kg
H – efficiency or performance
h – specific enthalpy, kJ/kg
I – irreversibility, KW
K – ratio of specific heats ($= C_p/C_v$)
L – length of the mixing chamber, m
M – Mach number
m – mass flow rate, kg/s
Q – heat load rate, kW
P – pressure, Pa
R – ideal gas constant (J/kgK)
r – compression ratio
S – cross-section area, m^2
S – specific entropy, kJ/kgK
T – temperature, K
T_0 – environmental temperature, K
T_b – temperature of the boiler
T_c – temperature of the condenser
T_g – temperature of secondary fluid in the boiler, K
T_h – temperature of secondary fluid in the condenser, K
T_r – temperature of secondary fluid in the evaporator, K
U – entrainment ratio of the ejector
X – position of the primary nozzle relative to the secondary nozzle throat, m
$\dot{w}_p$ – pump power
$\dot{w}_c$ – compressor power
U – entrainment ratio
V – velocity, m/s
$\dot{W}$ – mechanical work rate, kW

Greek symbols

η_{II} – second law efficiency, %
ϕ – area ratio between mixing tube and primary nozzle throat ($= (D/d_x)^2$)
ξ – driving pressure ratio
Δ – related to the variation of a parameter
ρ – density, kg/m^3
η – compressor efficiency, %

Exponents and Subscripts

c – compressor
e – evaporator

B – boiler
Ev – expansion valve
Int – intercooler
cd – condenser
Ej – ejector
D – diffuser
p – pump
$*$ – primary nozzle throat
$'$ – primary fluid (or motive fluid)
$''$ – secondary fluid (or entrained aspirated)

1 Introduction

Many industrial sectors (food, chemical, and pharmaceutical) require low temperature cooling and high temperature heating simultaneously which cannot be achieved simultaneously and effectively by single stage or multi-stage systems due to individual limitation of refrigerant. These needs can be achieved by using a cascade system.

Bhattacharyya *et al.* [1] examined CO_2-C_3H_8 cascade system for simultaneous refrigeration at -40 °C and heating at 80 °C. A parametric study on NH_3-CO_2 cascade refrigeration system was reported for a temperature range of -50 to 40 °C [2]. Bhattacharyya *et al.* [3] analyzed a natural refrigerant based cascade system with nitrous oxide as the low temperature fluid and carbon dioxide as the high temperature fluid for simultaneous cooling and heating applications. They found that for a given set of operating parameters the optimized intermediate temperature for a maximum coefficient of performance (COP) varies with the approach temperatures of the gas cooler and the evaporator in such a way that the nitrous oxide condensing temperature in cascaded heat exchanger remains the same. They found also that the system performance is independent of fluids used in high temperature and low temperature cycles, since N_2O and CO_2 have very similar thermodynamic properties.

Using low temperature energy source applications such as solar energy, geothermal energy and waste heat for simultaneous refrigeration and heating applications is the primary objective of the present study. This paper describes a hybrid system that combines a basic compression heat pump cycle with an ejector cooling cycle. The interface between both systems is an intercooler. A schematic diagram of the combined system is shown in Fig. 1. The pressure-enthalpy diagram is presented in Fig. 2. For thermodynamic reasons, the working fluid exiting the compressor providing a considerable

thermal energy and exergy which will be dissipated if not used. This is an ideal thermal energy source to be used in heating application or for power generation. To our knowledge, this sort of waste heat utilization has not been investigated yet and worth to be paid attention. In particular, there is a lack of knowledge when this heat utilization is performed in a cascade system with an ejector.

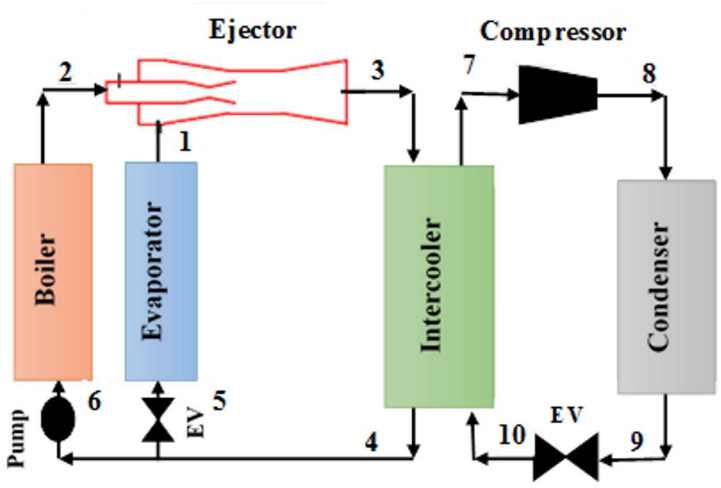

Figure 1: Schematic of the cascade cycle for refrigeration and heating.

Many hydrofluorocarbon (HFC) refrigerants and natural fluids will be analyzed in this cycle to find the most suitable fluid that allows the highest performance. To ameliorate this system we analyze thermodynamic models with ejectors. We will use a one dimensional based on the constant area mixing ejector at critical mode. To locate sources of losses, we will investigate the behavior of the cascade system using the exergy method.

The refrigeration and heat pump cascaded system has been modeled employing energy conservation on each individual component of the system. The following assumptions have been made to simplify the analysis:

1. Heat transfer in heat exchanger with the ambient is negligible.
2. The compression process in the compressor is adiabatic and irreversible.
3. The expansion process is isenthalpic.
4. Pressure drop in the connecting pipes and heat exchangers are negligible.

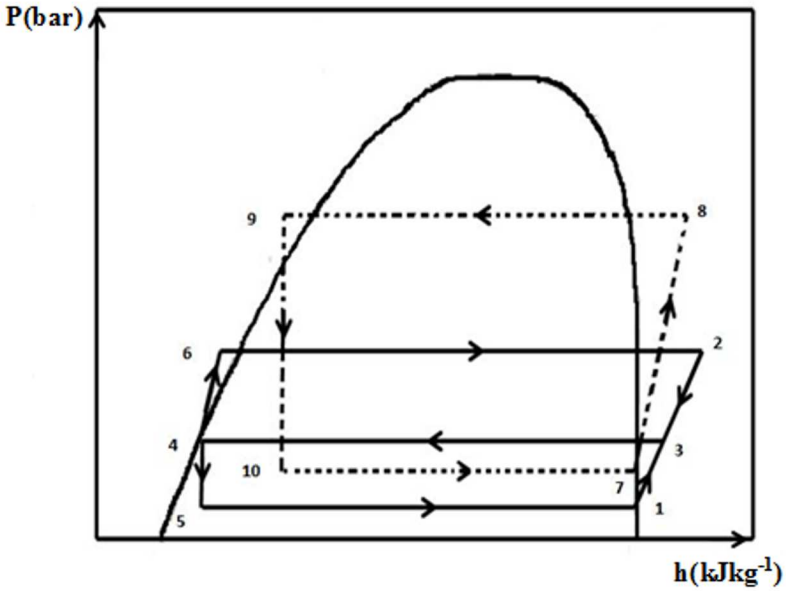

Figure 2: Pressure-enthalpy (p-h) diagram for the cascade cycle for refrigeration and heating.

2 Energetic analysis

The ejector entrainment ratio, $U = m_1/m_2$ is defined as the ratio of the ejector suction mass flow rate at state (1) to the motive mass flow rate at state (2). For a mass flow rate of 1 kgs^{-1} refrigerant mixture in the ejector, the suction and motive mass flow rate will be $U/(U+1)$ $\mathrm{kg\,s}^{-1}$ and $1/(1+U)$ kgs^{-1}, respectively. The compressors consumption powers, the heat load rate and the absorbed heat are defined by the following expressions:

$$\dot{W}_{comp} = \dot{m}_1(h_8 - h_7)\ , \tag{1}$$

where

$$h_8 = h_7 + \frac{(h_{8is} - h_7)}{\eta_s}\ , \quad h_{8is} = h_{8is}\ (P = P_9,\ s = s7)$$

The compressor efficiency η_s is given by Brunin *et al.* [11] as

$$\eta_s = 0.874 - 0.0135\frac{P_8}{P_7}\ ,$$

$$\dot{W}_p = (h_6 - h_4)\frac{1}{1+U} \,, \tag{2}$$

$$\dot{Q}_e = (h_1 - h_5)\frac{U}{1+U} \,, \tag{3}$$

$$\dot{Q}_b = (h_2 - h_6)\frac{1}{1+U} \,, \tag{4}$$

$$\dot{Q}_{cd} = \dot{m}_1 (h_8 - h_9) \,. \tag{5}$$

The energy balance at the cascade heat exchange is expressed by

$$h_3 - h_4 = \dot{m}_1 (h_7 - h_{10}) \,, \tag{6}$$

$$\dot{m}_1 = \frac{h_3 - h_4}{h_7 - h_{10}} \,. \tag{7}$$

The system performance could be evaluated using its coefficient of performance, which is defined as

$$COP = \frac{\dot{Q}_e + \dot{Q}_{cd}}{\dot{Q}_b + \dot{W}_{comp} + \dot{W}_p} \,. \tag{8}$$

3 Ejector modeling

The ejector consists of two nozzles: a primary nozzle also called the driving nozzle, secondary nozzle, mixing tube and diffuser [4,5]. In the driving nozzle, the enthalpy of the fluid is converted into kinetic energy. At the output of the driving nozzle, the jet velocity is very high, causing a negative pressure around the outlet section.

At the same time, due to a strong interaction between the two jets, resulting in exchange of mass and momentum, fluid from the secondary nozzle is sucked and brought by the primary fluid, producing entrainment phenomenon. The mixing process takes place in the mixing chamber, producing a kinetic energy transformation of the jet engine into enthalpy of the mixture and therefore by an increase in the pressure of the latter. At the outlet of the mixing chamber, the fluids sufficiently mixed pass through the diffuser, in which there will be a conversion of kinetic energy into pressure.

Le Grives and Fabri defined three different operating regimes for ejectors [6]. In these definitions, the ejector operating regimes are named based on the dependence of the entrainment ratio on the back pressure at the exit

of the ejector (or the driving pressure ratio). These regimes are the supersonic regime (SR), the transition regime (TR) and the mixed regime (MR). The performance analysis of an ejector consists of determining the formation conditions of these regimes. During the operation of ejector in the SR, since the primary static pressure at section e_1 shown in Fig. 3, is higher than that of the secondary vapor, the primary fluid expands against the secondary fluid and causes the velocity of the secondary fluid to reach supersonic speed at the aerodynamic throat formed by it. As a consequence of this secondary stream choking phenomenon, the secondary mass flow rate becomes independent of the back pressure. The MR includes all the cases for which the secondary flow is not choked. The secondary flow cannot reach sonic speed within the mixing chamber, and therefore, its mass flow rate changes depending on the back pressure. In the TR, the secondary vapor reaches supersonic speed at the point of confluence of the primary and secondary vapours. It gives the optimum performance of the ejector [7]. For this reason, we will analyze the ejector in TR. The ejector modeling in transition regime developed by [8] by using the one-dimensional constant-area ejector model is modified so that it could be applied to the ejector-compression cycle for cogeneration of heat and cold.

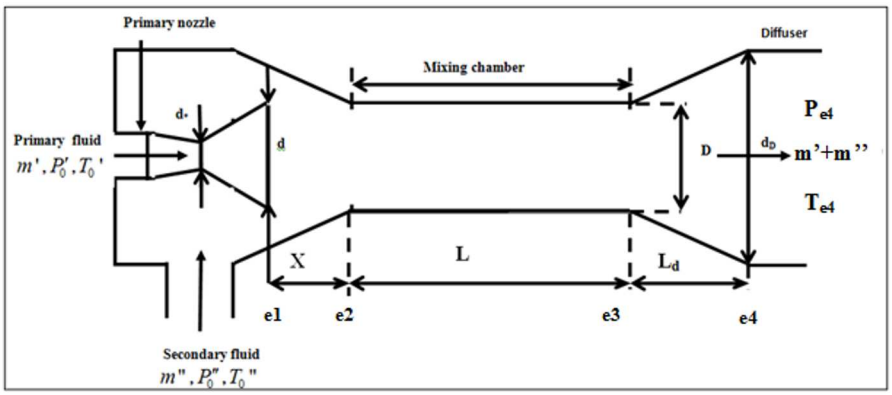

Figure 3: Schematic of a constant-area ejector and geometric parameters [9].

The following assumptions are made for the analysis:

1. The flow inside the ejector is considered one-dimensional homogeneous equilibrium flow.
2. The working fluid is an ideal gas with constant properties C_p and k.

3. For simplicity in deriving the 1D model, the isentropic relations are used before mixing.
4. The two fluids are completely mixed at the exit of the mixing chamber.
5. $X \neq 0$.
6. Kinetic energies of the refrigerant at the ejector inlet and outlet are negligible.

With $X \neq 0$ the flow in convergent part is sonic which implies that the aerodynamic throat is situated in the cylindrical part of the mixing chamber. So, we deduce that, for TR with a distance $X \neq 0$, the aerodynamic throat is located at the entry of the mixing chamber. Therefore

$$M''_{e2} = 1 \, . \tag{9}$$

To form the sonic throat of the secondary fluid at the section e_2, the motive flow must expand, which imposes $P'_{e2} > P''_{e2}$. After the section e_2, we can only have $P'_{e2} > P''_{e2}$, since the case $P'_{e2} < P''_{e2}$, is physically impossible. For the condition $P'_{e2} > P''_{e2}$, the primary fluid is going to continue to expand, the sonic throat is situated then downstream the section e_3 and the regime becomes supersonic. Therefore, the TR is characterized by

$$P'_{e2} = P''_{e2} \, . \tag{10}$$

By applying the mass, momentum and energy balances to the control volume defined between section e_2 and section e_3, we can write the following equations:
continuity equation

$$m' + m" = m_3 \tag{11}$$

with

$$U = \frac{m"}{m'} \, . \tag{12}$$

The Eq. (11) can be expressed as

$$\frac{m_3}{m'} = 1 + U \, . \tag{13}$$

Energy equation

$$m' C_p T'_0 + m" C_p T_0" = m_3 C_p T_{0e3} \, , \tag{14}$$

where T_{0e3} is the stagnation temperature at the section e_3.

By dividing the two members of the equation by $m'C_pT_0^{'}$, the energy equation can be expressed as follows:

$$(1+U\theta) = (1+U)(\frac{T_{0e3}}{T_0'}) \ , \tag{15}$$

where θ is defined as

$$\theta = \frac{T_0"}{T_0'} \ . \tag{16}$$

Momentum equation

$$m_{e3}V_{e3} + P_{e3}S_{e3} + \Delta PS_{e3} = m'V_{e2}' + P_{e2}'S_{e2}' + m"V_{e2}" + P_{e2}"S_{e2}" \tag{17}$$

where ΔPS_{e3} expresses the frictional losses inside the mixing chamber and is obtained from the following equation:

$$\Delta PS_{e3} = F(\frac{\rho V_m^2}{2})(\frac{L}{D})S_{e3} \ , \tag{18}$$

where F is the friction factor. With the assumption $\rho V_m^2 = \rho_{e3}V_{e3}^2$, Eq. (18) can be expressed as

$$\Delta PS_{e3} = F(\frac{L}{D})m_{e3}\frac{V_{e3}}{2} \ . \tag{19}$$

In order to simplify the equations resolution, the dimensionless velocity M ($M = V\ /a_*$) and the new function, $f_1(M)$, are introduced:

$$f_1(M) = \frac{1}{M} + M \ , \tag{20}$$

where a_* is the sound speed at the nozzle throat and it is given by

$$a_* = \sqrt{kRT_*}$$

and after a series of transformations of the expression $MV + PS$ we obtain

$$MV + PS = \frac{k+1}{2k}a_*mf_1\left(M\right) \ . \tag{21}$$

By using Eqs. (19) and (21) and by dividing the momentum equation, Eq. (17) by $\frac{k+1}{2k}a_*'m'$, finally Eq.(17) can be expressed as

$$\frac{a_{*e3}}{a_*'}\frac{m_{e3}}{m'}\Big[f_1(M_{e3}) + xM_{e3}\Big] = f_1(M_{e2}') + \frac{a_*"}{a_*'}\frac{m"}{m'}f_1(M_{e2}") \ , \tag{22}$$

where x is defined as $x = \frac{k}{k+1}\frac{L}{D}F$.

The distance L (Fig. 3) in the TR is assumed to be 10 D. By using the isentropic relations, the momentum equation becomes:

$$\left(1 + U\,(\theta)^{\frac{1}{2}}\right)\left[f_1(M_{e3}) + xM_{e3}\right] = f_1(M'_{e2}) + U\,(\theta)^{\frac{1}{2}}\, f_1(M_{e2}")\,. \tag{23}$$

Calculation of the stagnation pressure P_{0e3} in the section e_3: The primary mass flow rate can be expressed as

$$m' = P'_0\frac{1}{\sqrt{T'_0}}S'_*\left(\frac{k}{R}\right)^{\frac{1}{2}}\left(\frac{2}{k+1}\right)^{\frac{k}{k-1}}\left(\frac{k+1}{2}\right)^{\frac{1}{2}}\,. \tag{24}$$

The mass flow rate in the section e_3 is

$$m_{e3} = P_{0e3}\frac{1}{\sqrt{T_{0e3}}}S_{*e3}\left(\frac{k}{R}\right)^{\frac{1}{2}}\left(\frac{2}{k+1}\right)^{\frac{k}{k-1}}\left(\frac{k+1}{2}\right)^{\frac{1}{2}}\,, \tag{25}$$

where S_{*e3} is the fictitious throat in the mixing chamber and can be expressed as follows by using isentropic relations:

$$S_{*e3} = S_{e3}f_2\,(k, M_{e3})\,, \tag{26}$$

where

$$f_2\,(k, M) = \frac{S_*}{S} = \left(\frac{k+1}{2}\right)^{\frac{1}{k-1}} M\left(1 - \frac{k-1}{k+1}M^2\right)^{\frac{1}{k-1}}\,. \tag{27}$$

By using Eq. (24) attributed to the section e_2 and Eq. (25), we obtain

$$\frac{m_{e3}}{m'_{e2}} = \frac{P_{0e3}}{P'_0}\left(\frac{T'_0}{T_{0e3}}\right)^{\frac{1}{2}}\frac{S_{e3}}{S'_*}f_2(k, M_{e3})\,. \tag{28}$$

Therefore

$$\frac{P_{0e3}}{P'_0} = \frac{1 + U\,(\theta)^{\frac{1}{2}}}{\Phi f_2(k, M_{e3})}\,, \tag{29}$$

where $\Phi = \frac{S_{e3}}{S'_*}$. Calculation of the static pressure P_{e4} in the section e_4: By using isentropic relations we can write

$$P_{e4} = P_{0e4}\left(1 - \frac{k-1}{k+1}M^2\right)^{\frac{k}{k-1}}\,, \tag{30}$$

where

$$f_3(k,M) = \left(1 - \frac{k-1}{k+1}M^2\right)^{\frac{k}{k-1}} \ . \tag{31}$$

We can also write

$$P_{e4} = P_{0e3}\eta_D f_3\left(k, M_{e4}\right) \ , \tag{32}$$

where η_D is the pressure coefficient in the diffuser and is expressed by

$$\eta_D = \frac{P_{04}}{P_{03}} \ . \tag{33}$$

By using a relation similar to Eq. (16) the mass flow rate at the exit of the diffuser can be expressed as

$$m_4 = P_{0e4}\frac{1}{\sqrt{T_{0e4}}}S_{e4}\left(\frac{k}{R}\right)^{\frac{1}{2}}\left(\frac{2}{k+1}\right)^{\frac{k}{k-1}}\left(\frac{k+1}{2}\right)^{\frac{1}{2}} f_2\left(k, M_{e4}\right) \ . \tag{34}$$

By combining Eqs. (25), (26), and (34) we obtain

$$\frac{m_{e4}}{m_{e3}} = \frac{P_{0e4}}{P_{0e3}}\left(\frac{T_{0e3}}{T_{0e4}}\right)^{\frac{1}{2}}\frac{S_{e4}}{S_{e3}}\frac{f_2(k,M_{e4})}{f_2(k,M_{e3})} \ . \tag{35}$$

The heat loss in the diffuser is neglected; the energy conservation in the diffuser imposes

$$m_3 C_p T_{03} = m_4 C_p T_{04} \ . \tag{36}$$

Therefore the stagnation temperatures T_{03} and T_{04} are equal. By using Eqs. (33), and (36) in (34) we obtain

$$f_2\left(k, M_{e4}\right) = \frac{f_2(k,M_{e3})}{\Omega\eta_D} \ , \tag{37}$$

where

$$\Omega = \frac{S_{e4}}{S_{e3}} \ .$$

Substituting Eqs. (29) and (29) in Eq. (32), we can find a relation between the exit parameters (P_{e4}, M_{e4}) and the inlet parameters (P'_0, θ):

$$\frac{f_2(k,M_{e4})}{f_3(k,M_{e4})} = \xi\frac{\left(1+U\left(\theta\right)^{\frac{1}{2}}\right)}{\Phi\Omega} \ . \tag{38}$$

Entrainment ratio U: Similar to Eq. (28), the entrainment ratio U can be expressed as

$$U = \frac{m"}{m'} = \frac{P_0''}{P_0'}\left(\frac{T_0'}{T_0''}\right)^{\frac{1}{2}} \frac{S_{e2}''}{S_*'} f_2(k, M_{e2}'') \,. \tag{39}$$

Finally, by using Φ we obtain

$$U\theta^{\frac{1}{2}} = \frac{P_0''}{P_0'}\left(\Phi - \frac{1}{f_2(k, M_{e2}')}\right) f_2(k, M_{e2}'') \,. \tag{40}$$

On the other hand, by using the hypothesis expressed by $P_{e2}' = P_{e2}''$, and similarly to Eq. (32), we have

$$P_{e2}' = P_0' f_3(k, M_{e2}')$$

and

$$P_{e2}'' = P_0'' f_3(k, M_{e2}'') \,,$$

hence

$$\frac{P_0'}{P_0'} = \frac{f_3(k, M_{e2}'')}{f_3(k, M_{e2}')} \,. \tag{41}$$

By combining Eqs. (40) and (41) we get

$$\frac{f_2(k, M_{e2}'')}{f_3(k, M_{e2}'')} = \frac{U\,(\theta)^{\frac{1}{2}}}{(\Phi - \frac{1}{f_2(k, M_{e2}')}) f_3(M_{e2}')} \,. \tag{42}$$

System of equations: The final system of equations used for the transition regime is given by

$$\left(1 + U\,(\theta)^{\frac{1}{2}}\right)\left[f_1(M_{e3}) + xM_{e3}\right] = f_1(M_{e2}') + U\,(\theta)^{\frac{1}{2}}\, f_1(M_{e2}'') \,, \tag{43}$$

$$f_2(k, M_{e4}) \quad = \frac{f_2(k, M_{e3})}{\Omega \eta_D} \,, \tag{44}$$

$$f_2(k, Me_4) = f_3(k, M_{e4}) \xi \frac{(1 + U\,(\theta)^{\frac{1}{2}})}{\Phi\Omega} \,, \tag{45}$$

$$U\,(\theta)^{\frac{1}{2}} = \frac{1}{\Gamma}\left(\Phi - \frac{1}{f_2(k, M_{e2}')}\right) f_2(k, M_{e2}'') \,, \tag{46}$$

$$\Gamma = \left(\frac{2}{k+1}\right)^{(k/k-1)} \frac{1}{f_3(k, M_{e2}')} \,. \tag{47}$$

In which

$$\Gamma = \frac{P_0'}{P_0' P_0''} \,, \tag{48}$$

$$\xi = \frac{P_0'}{P_0' P_{e4}} \,, \tag{49}$$

$$r = \frac{P_{e4}}{P_{e4} P_0''} \,, \tag{50}$$

or

$$r = \frac{\Gamma}{\Gamma \xi} \,.$$

In this system of equations, we have nine parameters: $U\,(\theta)^{\frac{1}{2}}$, ξ, Γ, Φ, Ω, M_i', M_i", M_3, and M_4 (by supposing that the pressure coefficient in the diffuser η_D and the friction factor F (therefore x are fixed). The most important parameters are thermodynamic parameters $U\,(\theta)^{\frac{1}{2}}$, ξ, Γ and geometric parameters: Φ, and Ω. To have the solution of the system, it is necessary to fix four initial parameters. In our case, the four fixed variables are: M_{e2}'', Γ, Φ and Ω. The five unknown parameters are $U\,(\theta)^{\frac{1}{2}}$, ξ, M_{e2}', M_{e3}, and M_{e4}.

The aim of the ejector modeling is to find the back pressures the ejector and the entrainment ratio.

4 Exergetic analysis

Heat transfer between a thermodynamic system and the surroundings is the most important source of irreversibility. This irreversibility causes a degradation of the system performance. Exergy analysis is a powerful tool to locate this irreversibility. It expresses the maximum quantity of work that would be possible for withdrawal by means of a driving thermodynamic cycle.

Exergy losses or irreversibility are defined as the difference between the exergy inputs to the process and the exergy output.

The total exergy destruction rate of the cycle is considered as the sum of the exergy destruction rates in each component:

$$I_{tot} = I_c + I_e + I_{cd} + I_{ev1} + I_{int} + I_b + I_p + I_{ej} + I_{ev2} \,. \tag{51}$$

Table 1: Shows the component's irreversibility for the cascade system with two ejectors.

Subsystems	Exergy relations
Compressor	$I_c = T_0 \dot{m}_1 (s_2 - s_1)$
Evaporator	$I_e = \dot{m}_1 T_0 (s_4 - s_1 + (h_4 - h_1)/T_r)$
Intercooler	$I_{int} = T_0 [U(s_5 - s_6)/(1+U) + \dot{m}_1 (s_3 - s_2)]$
Expansion device1	$I_{ev1} = T_0 \dot{m}_1 (s_4 - s_3)$
Expansion device2	$I_{ev2} = T_0 (s_6 - s_7) U/1 + U$
Condenser	$I_{cd} = [h_{10} - h_7 - T_0 (s_{10} - s_7)]$
Ejector	$I_{ej} = T_0 [s_{10} - s_9/(1+U) - s_5 U/1 + U]$
Pump	$I_p = T_0 (s_7 - s_8)/(1+U)$
Generator	$I_b = T_0 [s_9 - s_8 + (h_8 - h_9)/T_g]/(1+U)$

The second-law efficiency, η_{II}, is a valuable parameter to evaluate the performance of cycle and can be expressed as follows:

$$\eta_{\mathrm{II}} = \frac{\dot{Q}_e (T_0/T_r - 1) + \dot{Q}_{cd} (1 - T_0/T_h)}{\dot{W}_c + \dot{W}_p} \,. \tag{52}$$

5 Validation of model results

Based on the above model a simulation program using the database REFPROP V 9.1 was developed. It determines the thermodynamic properties and the mass flow rate of working fluids at all the states identified in Fig. 1.

The validation of the computer simulation of the ejector vapor-compression cycle is carried out for R134a with $T_b = 78$ °C and $T_c = 40$ °C, by varying the intercooler temperature from 13 to 25 °C. The simulated performance is compared with that of experimental data available in the literature [10]. The simulated results agree fairly well with the experimental data, shown in Tab. 2, and the maximum deviation is found to be 6.06%.

Table 2: Comparison of the present model results with the experimentally validated results.

T_e (°C)	COP		Relative error (%)
	Jia *et al.* [10]	Present study	
13	3.5	3.7	5.71
16	3.4	3.6	5.88
19	3.3	3.5	6.08
22	3.25	3.4	4.61
25	3.19	3.3	3.44

6 Influence of fluid nature on exergy loss and system performance

For fixed operate conditions (T_e = 10 °C, T_c = 80 °C, T_b = 65 °C, T_r = 15 °C, T_0 = 25 °C, T_h = 75 °C, and T_g = 70 °C), the temperature difference in the intercooler between the two subcycles, ΔT, is assumed to be 5 °C [13,14], 2017). Several fluids have been studied to find the fluid which gives the maximum performance.

The refrigerants considered in this study are pure fluids. R1270, R125, R143a, R32, R41 show higher COP than R22. We found that the COP is improved by 3.84%, 4.7%, 4.27%, 8.97%, and 10.68% respectively (Fig. 4). Figure 5, shows the second law efficiency for various pure fluids. The R32 gives the best performance. To locate sources of losses, we investigate the behavior of cascade system using the exergy method. In Fig. 6, the exergy loss of R227ea, R236ea, R236fa, R32, Rc318, R134a, R1234yf, and R1234ze is clearly lower than for R22.

All in all and based in the energy and exergy analysis R32 still becomes the best choice to be used in this proposed system. The aim of this work is to study the performance of this fluid.

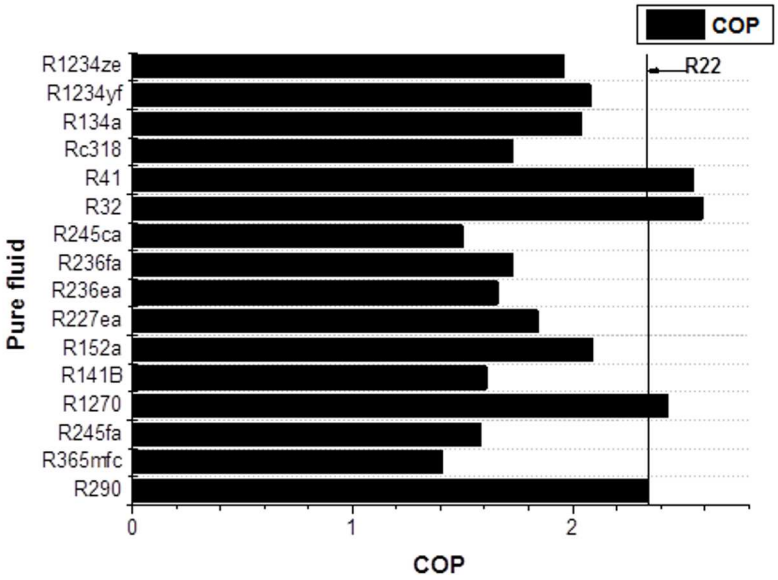

Figure 4: COP variation versus different pure fluids.

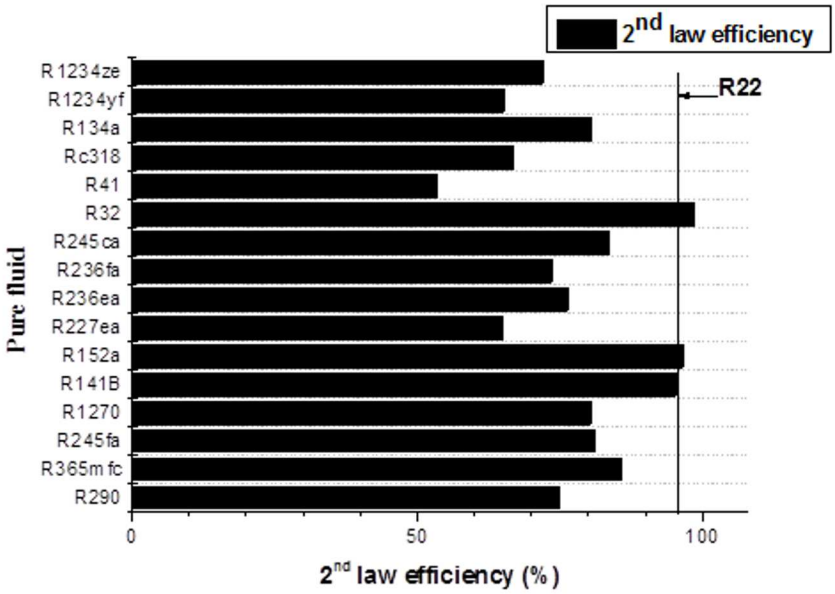

Figure 5: Second law efficiency variation versus different pure fluids.

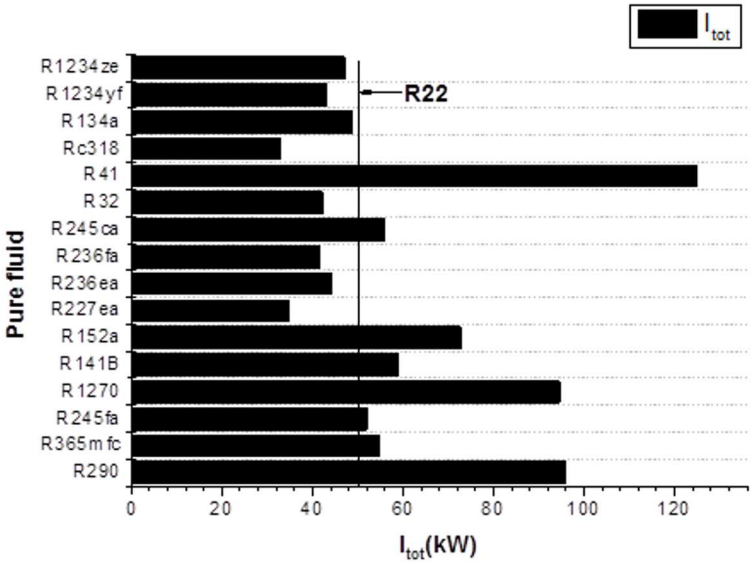

Figure 6: Total irreversibility loss variation versus different pure fluids.

7 Influence of condensation temperature on system performance and exergy loss

Figures 7 and 8 display the effect of the condensation temperature on the coefficient of performance and the second law efficiency of the system. The COP and the second law efficiency decrease with increasing condensation temperature, since the exergy loss of the overall system increases (Fig. 9). The exergy loss of each component for the R32 are plotted in Fig. 10. Remarkably, the exergy destruction rates of the components in the compressor heat pump except the intercooler grow while the others' tend to be constant.

The largest loss 39.19% occurs in the condenser followed by the expansion valve 8.66% for $T_c = 55$ °C. The rest of the exergy loss occurs in the compressor, pump, evaporator, ejector, intercooler and the boiler.

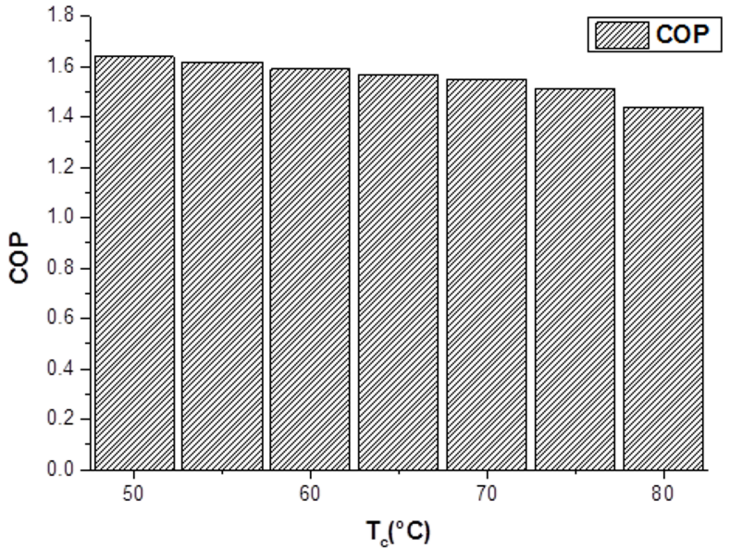

Figure 7: COP variation versus condensation temperature.

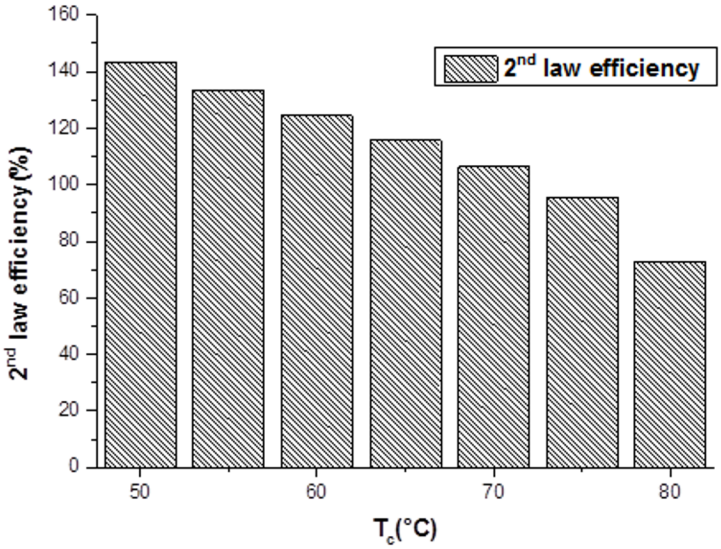

Figure 8: Second law efficiency variation versus condensation temperature.

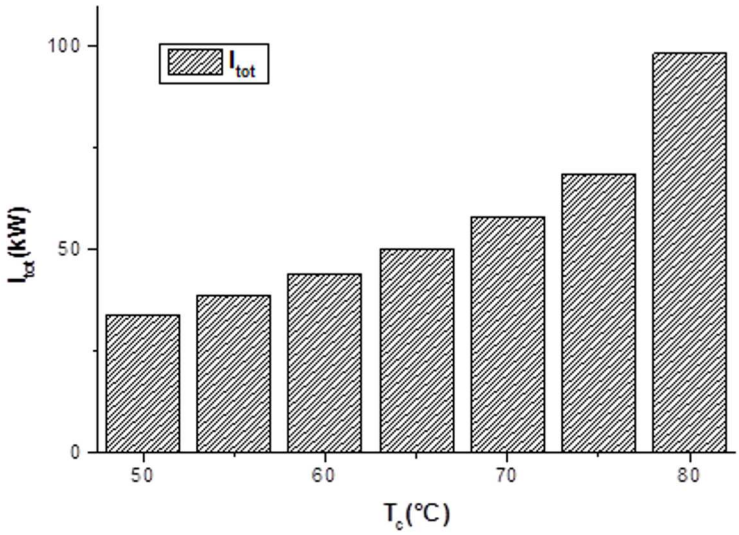

Figure 9: Total irreversibility loss variation versus condensation temperature.

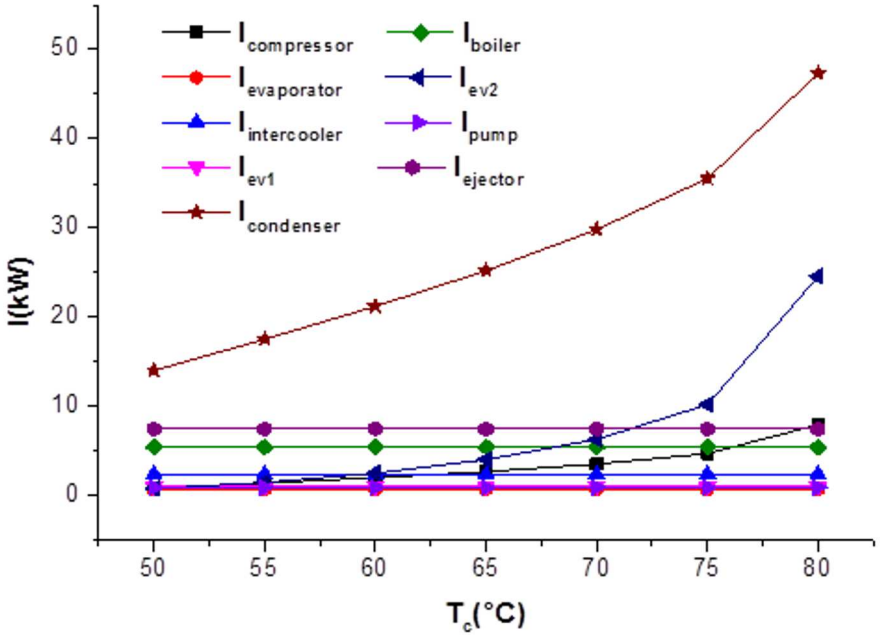

Figure 10: Effect of condensing temperature on exergy loss of each component (R32).

8 Influence of evaporation temperature system performance on exergy losses

The operating conditions are chosen such as $T_c = 75$ °C, $T_b = 90$ °C, and $\Delta T = 5$ °C. The temperature of evaporator is varied between -15 °C and 20 °C. It is observed that increasing the evaporation temperature increases COP (Fig. 11) however the total exergy loss decreases (Fig. 13). The Fig. 12 indicates that the evaporator temperature has less influence on the second law efficiency.

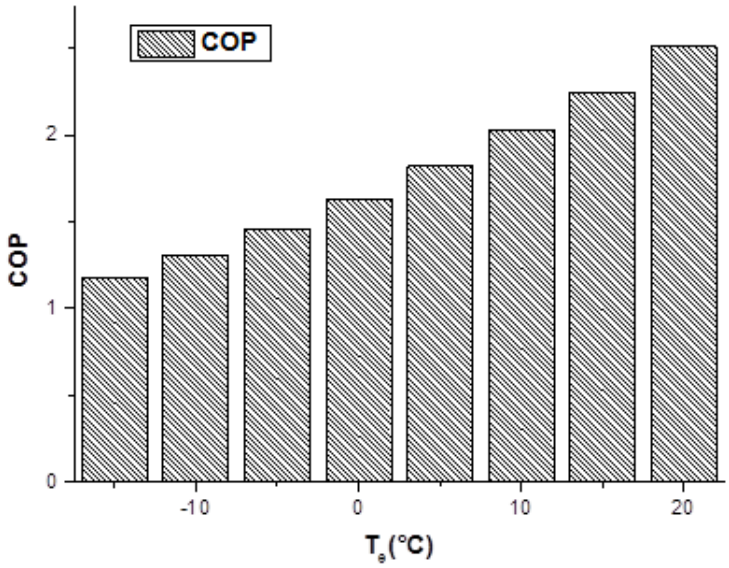

Figure 11: COP variation versus evaporating temperature

The exergy loss decreases in all components of the proposed cycle when the evaporation temperature rise from -15 to 20 °C. The decrease in the irreversibility in the condenser and the expansion valve (Fig. 14) decreases the overall irreversibility and consequently higher performance.

9 Conclusion

The impact of three design parameters has been studied, namely the condenser temperature, evaporator temperature, and the nature of fluid. The important conclusions which can be drawn from this study can be summa-

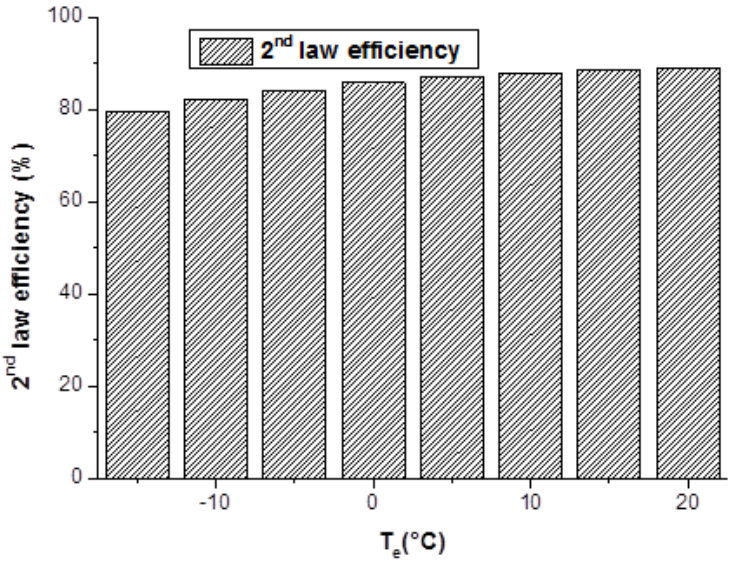

Figure 12: Second law efficiency variation versus evaporating temperature.

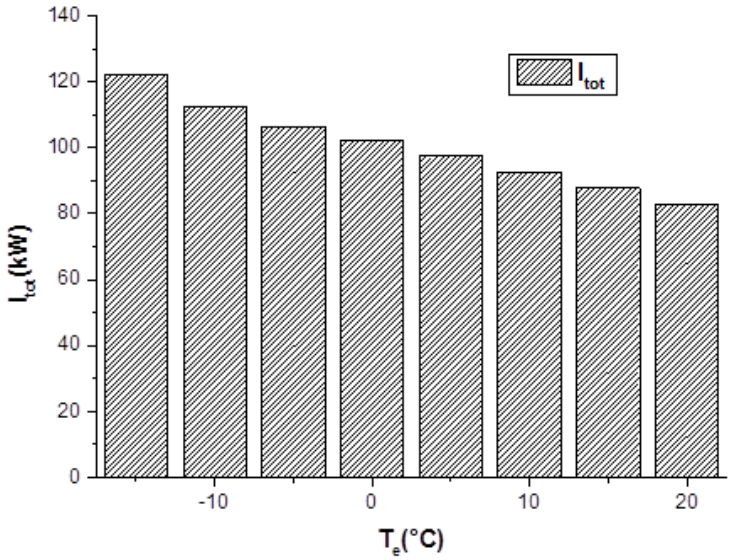

Figure 13: Total irreversibility loss versus evaporating temperature.

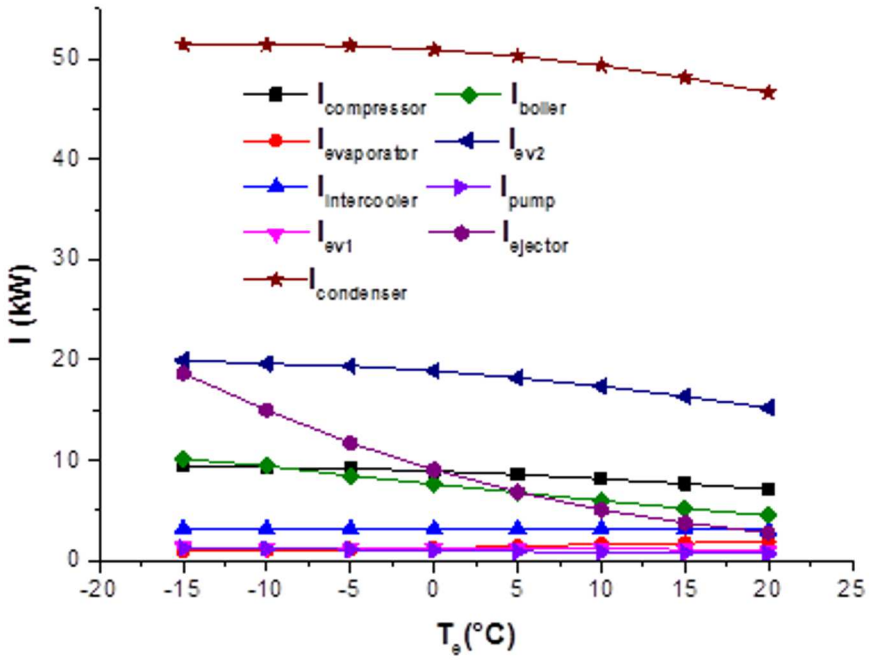

Figure 14: Effect of evaporating temperature on exergy loss of each component (R32).

rized as follows:

- It is observed that the coefficient of performance and the second law efficiency increased with the increasing evaporator temperature or decreasing the condenser temperature.
- Exergy analysis is good for finding the losses in the system.
- It is hoped that these theoretical results will stimulate wider interest in the technology of the application of R32 as an alternative refrigerant to R22 for refrigeration and heat pump applications.

Received April 2017

References

[1] Bhattacharyya S., Mukhopadhyay S., Kumar A., Khurana R.K., Sarkar J.: *Optimization of a CO_2-C_3H_8 cascade system for refrigeration and heating.* Int. J. Refrig. **28**(2005), 8, 1284–1292.

[2] Getu H.M., Bansal P.K.:. *Thermodynamic analysis of an R744–R717 cascade refrigeration system.* Int. J. Refrig. **31**(2008), 1, 45–54.

[3] Bhattacharyya S., Garai A., Sarkar J.: *Thermodynamic analysis and optimization of a novel N_2O-CO_2 cascade system for refrigeration and heating.* Int. J. Refrig. **32**(2009), 5, 1077–1084.

[4] Sokolov M., Hershgal D.: *Enhanced ejector refrigeration cycles powered by low grade heat. Part 1: Systems characterization.* Int. J. Refrig. **13**(1990), 6, 351–356.

[5] Sun D.W.: *Solar powered combined ejector-vapour compression cycle for air conditioning and refrigeration.* Energ. Convers. Manage. 38(1997), 5, 479–791.

[6] Le Grives E., Fabri J.: *Divers régimes de mélange de deux flux d'enthalpie d'arrêt différent.* Astronautica Acta **14**(1969), 203–213.

[7] Nahdi E., Champoussin J.C., Hostache G., Cheron J.: *Optimal geometric parameters of a cooling ejector compressor.* Int. J. Refrig. **16**(1993), 1, 67–72.

[8] Lu L.T.: *Etudes théorique et expérimentale de la production de froid par machine tritherme a éjecteur de fluide frigorigène'.* PhD thesis, Laboratoire d'Energétique et d'Automatique, de l'INSA de Lyon 1986.

[9] Megdouli K., Tashtoush B.M., Nahdi E., Elakhdar M., Kairouani L., Mhimid A.: *Thermodynamic analysis of a novel ejector cascade refrigeration cycles for freezing process applications and air-conditioning.* Int. J. Refrig. **70**(2016), 108–118.

[10] Yan J., Cai W., Zhao L., Li Y., Lin C.: *Performance evaluation of a combined ejector-vapor compression cycle.* Renew. Energ. **55**(2013), 331–337.

[11] Brunin O., Feidt M., Hivet B.: *Comparison of the working domains of some compression heat pumps and a compression-absorption heat pump.* Int. J. Refrig. **20**(1997), 5, 308–318.

[12] *REFPROP. Thermodynamic Properties Refrigerant Mixtures, Version 9.1.* NIST, (2006).

[13] Yari M., Mahmoudi S.M.S: *Thermodynamic analysis and optimization of novel ejector-expansion TRCC (transcritical CO_2) cascade refrigeration cycles (Novel transcritical CO_2 cycle).* Energy **36**(2011), 12, 6839–6850.

[14] Megdouli K., Tashtoush B.M., Ezzaalouni Y., Nahdi E., Mhimid A., Kairouani L.: *Performance analysis of a new ejector expansion refrigeration cycle (NEERC) for power and cold: Exergy and energy points of view.* Appl. Therm. Eng. **122**(2017), 39–48.